Journal of Geochemical Exploration 165 (2016) 23–34

Contents lists available at ScienceDirect

Journal of Geochemical Exploration

journal homepage: www.elsevier.com/locate/gexplo

Proposing drilling locations based on the 3D modeling results of fluid inclusion data using the support vector regression method

Maliheh Abbaszadeh [a,*], Ardeshir Hezarkhani [b], Saeed Soltani-Mohammadi [a]

[a] Department of Mining Engineering, University of Kashan, Kashan, I. R., Iran
[b] Department of Mining and Metallurgical Engineering, Amirkabir University of Technology, Tehran, I. R., Iran

ARTICLE INFO

Article history:
Received 13 August 2015
Revised 12 February 2016
Accepted 16 February 2016
Available online 18 February 2016

Keywords:
Fluid inclusion
Sungun porphyry copper deposit
Predictive model
Support vector regression (SVR)

ABSTRACT

In recent years, effort has been made to make the results of fluid inclusion studies applicable and use them in the design of the exploration process. It has been tried in this paper to propose a mineralization predictive model for chalcopyrite deposition based on favorable thermodynamic conditions using the 3D modeling results of the fluid inclusion data. To study the applicability and efficiency of the proposed method, Sungun porphyry copper deposit, East Azarbaijan province, Iran, was studied as a case and the 3D model of the fluid inclusion data was prepared using the support vector regression method. The model precisions for the estimation of the fluid inclusion data including homogenization temperature, eutectic temperature and salinity were respectively 76, 71, and 93%. The predictive model was prepared based on the chalcopyrite deposition's favorable thermodynamic conditions (a homogenization temperature range of 300–400 °C and moderate-to-high salinity). A comparison of the predictive model with that of the copper grade shows the efficiency of the proposed modeling and high conformity of the two models. The drilling pattern was then investigated based on the predictive model and showed that there would be an almost 6% cost reduction (i.e. elimination of 9 drillholes) if use was made of the proposed predictive model in the design of exploration drillholes.

1. Introduction

In recent years, fluid inclusion studies have become very popular with the researchers and quite common in economic geology studies and mineral exploration. The fluid inclusion data modeling literature can be divided into three points: 1) physicochemical modeling of the fluid inclusion data (e.g., Jadhav et al., 1993; Bakker, 1999; Hezarkhani, 2006b; Moritz, 2006; Thiery, 2006; Zhang et al., 2007; Canet et al., 2011), 2) alteration zones modeling based on the fluid inclusion data (Hezarkhani, 1997; Tahmasebi and Hezarkhani, 2009; El-Makky, 2011; Abbaszadeh et al., 2013; Abbaszadeh et al., 2015), and 3) the 3D modeling of the fluid inclusion data (Sun et al., 2011). The first group of literature on fluid inclusion data modeling has been more favored because: a) the related studies are numerous and the date goes back to the 1900s (e.g., Jadhav et al., 1993; Bakker, 1999) or earliear, and b) due to different fluid inclusion thermodynamic conditions, this type of modeling has been done on a variety of such mineral deposits as porphyry copper (Rusk et al., 2004; Landtwing et al., 2005; Hezarkhani, 2006b; Hezarkhani, 2006a; Hezarkhani, 2008b; Hezarkhani, 2009), epithermal (Moritz, 2006; Canet et al., 2011), polymetallic (Zhang et al., 2007), intrusion-related gold (Abdollahi et al., 2009), and hydrocarbon deposits (Thiery, 2006). The main method of modeling and identification of alteration zones is through petrography and mineralography where the identification and discrimination of alteration zones are done through direct observations and identification of the index minerals. So far, few research studies have been done on indirect modeling of alteration zones. In these studies, the identification and discrimination of alteration zones have been done based on indirect observations (i.e., parameters obtained from fluid inclusion or whole rock geochemical studies (Hezarkhani, 1997)) using numerical modeling methods such as neural networks (Hezarkhani et al., 2010), support vector machines (Abbaszadeh et al., 2013, 2015), principal component analysis (Tahmasebi and Hezarkhani, 2009), and discriminant analysis (Asghari and Hezarkhani, 2008). Since identification of alteration zones, as a grade control parameter, is a key process in preliminary and detailed exploration of porphyry deposits (Beane and Bodnar, 1995), the major part of these studies is related to such deposits (Lowell and Guilbert, 1970; Beane and Titley, 1981).

In 3D modeling of fluid inclusion data (homogenization temperature, eutectic temperature, salinity, etc.), the only study worth mentioning is that of Sun et al. (2011) wherein a 3D model of fluid inclusion data of China's Caixiashan Pb and Zn deposit has been prepared using inverse distance weighting (IDW) and compared with

* Corresponding author.
E-mail address: Abbaszadeh@kashanu.ac.ir (M. Abbaszadeh).

http://dx.doi.org/10.1016/j.gexplo.2016.02.005
0375-6742/

the ore-forming anomaly elements. Sun et al. (2011) have shown that such 3D models can be used in ore genesis and mineral exploration studies. Although IDW is a simple and common estimation method, it is not considered as robust and effective because it considers only the distance between the samples and the point being estimated. Effort has been made in this paper to enhance the estimation quality through machine learning algorithms and to use the results in such exploratory decision making as locating additional drillholes. The general characteristic of such algorithms is to emphasize the fact that they can estimate any multivariable nonlinear relationship among variables through their black-box-like performance. Another merit of such methods is their high capability in dealing with small data sets and error-tainted data (Zhang et al., 1998; Dutta, 2006).

A machine learning algorithm, famous in different scientific branches for estimation and prediction, is the support vector machine which, despite its newness, has gained widespread acceptance in a short period of time due to its robust mathematical background (Smola and Scholkopf, 1998; Kecman, 2000, 2004; Smola and Scholkopf, 2004).

The history of research on using modeling techniques for locating drillholes goes back to the research of Drew (1974) on drillholes' network design (drilling pattern and drillholes spacing) aimed at enhancing exploration probability. Then, based on that research, extensive research was performed in 2D (Savinskii, 1965; Koch and Link, 1974) and 3D (Malmqvist et al., 1980; Schuenemeyer et al., 1980) space for exploration of petroleum (Drew, 1974) and mineral (Koch and Link, 1974) reserves. With the development of geostatistics, many of the subsequent studies on locating additional drillholes tried to minimize the estimation variance (Kim et al., 1981; Chou and Schenk, 1983). The main difference between these methods is in defining the objective function (Gershon, 1983; Szidarovszky, 1983; Soltani and Hezarkhani, 2011; Morshedy and Memarian, 2015; Morshedy et al., 2015) and in the solution method (Soltani et al., 2011; Soltani Mohammadi et al., 2012). The proposed objective functions are all functions of kriging variance as the total kriging variance (Chou and Schenk, 1983; Gershon, 1983; Szidarovszky, 1983), weighted average kriging variance with respect to grade (Hassani Pak and Sharafodin, 2004; Soltani Mohammadi et al., 2012; Morshedy and Memarian, 2015; Morshedy et al., 2015), statistical value of information (Soltani and Hezarkhani, 2013a) and real value of information (Soltani-Mohammadi and Hezarkhani, 2013b). The solution methods used in this regard include the branch and bond algorithm (Szidarovszky, 1983), simulated annealing algorithm (Soltani and Hezarkhani, 2013a), and genetic algorithm (Soltani et al., 2011). The common weak point of all these locating algorithms is that their outputs depend only on the locations of the initial drillholes and the parameters of variogram model; they are incapable of utilizing other data gathered in the process of exploration. Emphasizing the necessity of utilizing other available relevant data in locating drillholes, Qahwash (1987) presented a method for defining optimal location and depth of drillholes based on geophysical data. Moncada (2008) has also pointed out the possibility of using fluid inclusion data in the exploration process management. In this paper, effort has been made to propose the locations of the additional drillholes based on a 3D model of fluid inclusion data.

2. Study area

The Sungun porphyry copper deposit (PCD) is located in East Azarbaijan province, northwest of Iran (Fig. 1). The magmatic suites in this area are part of the NW–SE trending Cenozoic magmatic belt of Iran and the porphyries occur as stocks and dikes (Hezarkhani, 2002; Calagari, 2003; Hezarkhani, 2003). This PCD is hosted in a diorite/granodiorite to quartz-monzonite stock that intrudes Eocene volcano-sedimentary and Cretaceous carbonate rocks (Hezarkhani et al., 1999). The porphyry stocks are divided into groups I and II. The latter, which hosts the Sungun PCD, ranges in composition from quartz monzonite through granodiorite to granite (Hezarkhani, 2002; Calagari, 2003; Hezarkhani, 2003) and has experienced multiple intense hydrofracturings manifested by numerous and varied crosscutting veinlets and microveinlets (Calagari, 2004). The main vein groups identified in Sungun are (Hezarkhani and Williams-Jones, 1998): 1) quartz + molybdenite + anhydrite ± K-feldspar with minor pyrite, chalcopyrite, and bornite, 2) quartz + chalcopyrite + pyrite ± molybdenite, 3) quartz + pyrite + calcite ± chalcopyrite ± anhydrite (gypsum) ± molybdenite, and 4) quartz ± calcite ± gypsum ± pyrite. In Sungun, three distinct types of hydrothermal alteration and mineralization are recognizable (Calagari, 2004): 1) hypogene, 2) contact metasomatic, and 3) supergene. The hypogene alterations developed in Sungun porphyries are: 1) potassic, 2) potassic–phyllic (transition), 3) phyllic, and 4) propylitic. The early hydrothermal alterations had been dominantly potassic and propylitic, which were then followed by later transition and phyllic alteration zones. The hypogene copper mineralization was introduced during the potassic, and to a lesser extent phyllic, alteration, and exists as disseminations in a veinlet form. During the potassic alteration, the hypogene copper mineralization consisted first of chalcopyrite and minor bornite and later mainly of chalcopyrite (Hezarkhani and Williams-Jones, 1998).

In general, fluid inclusions are classified, based on the number, nature, and proportion of the existing phases at room temperature, into three main types. The LV inclusions contain liquid + vapor ± solid phases (with the liquid phase dominating volumetrically). These fluid inclusions contain considerable mineralization in all quartz veins with the most plentitude in vein groups 2 and 3. The VL inclusions contain vapor + liquid ± solid phases (with the vapor phase dominating volumetrically). The LVHS inclusions are multiphase and consist of liquid + vapor + halite + other solids, and are divided into three subgroups ($LVHS_1$, $LVHS_2$ and $LVHS_3$), based on the number and type of solids (Hezarkhani and Williams-Jones, 1998).

Fluid inclusions in Sungun copper deposit can be classified into three populations. Population I includes $LVHS_1$, $LVHS_2$, and VL types, which are formed mainly in quartz veins of groups 1 and 2 of the potassic alteration zone (35 to 500 m below the existing erosion surface), but are rare in shallow levels in the phyllic alteration zone. These inclusions express the earliest episode of fluid entrapment in Sungun deposit. Population II inclusions pertain to shallower levels, where is a close spatial association of solid-rich $LVHS_3$ and VL fluid inclusions in the phyllic alteration zone. These fluids, found together in growth zones, are generally formed along the healed fractures. Population III includes LV fluid inclusions formed in all vein groups, but the phyllic and propylitic alteration zones have the highest plentitude in the veins of groups 2 and 3; they lie, quite clearly, along the fracture planes and are secondary in origin (Hezarkhani and Williams-Jones, 1998).

3. Materials and methods

3.1. Support vector regression (SVR)

The SVR, which is based on the statistical learning theory and the structural risk minimization, was first introduced by Vapnik (1995). So far, few research studies have been done regarding the application of SVR with spatial data, among which mapping of natural radioactivity (Pozdnoukhov, 2005), estimation of the arsenic concentration in stream sediments (Twarakavi et al., 2006), classification of lithology from well logs (Al-Anazi and Gates, 2010), mineral prospectivity mapping (Zuo and Carranza, 2011; Geranian et al., 2015) and grade and ore reserve estimation (Dutta et al., 2010; Chatterjee and Bandopadhyay, 2011) are worth mentioning.

Based on SVR, for the given training sample $D=\{(x_i,y_i)|x\in R^d, y_i\in R, i=1,2,\ldots,n\}$, through the non-linear mapping function $\varphi(x)$, the sample data x is mapped to another high dimensional feature space;

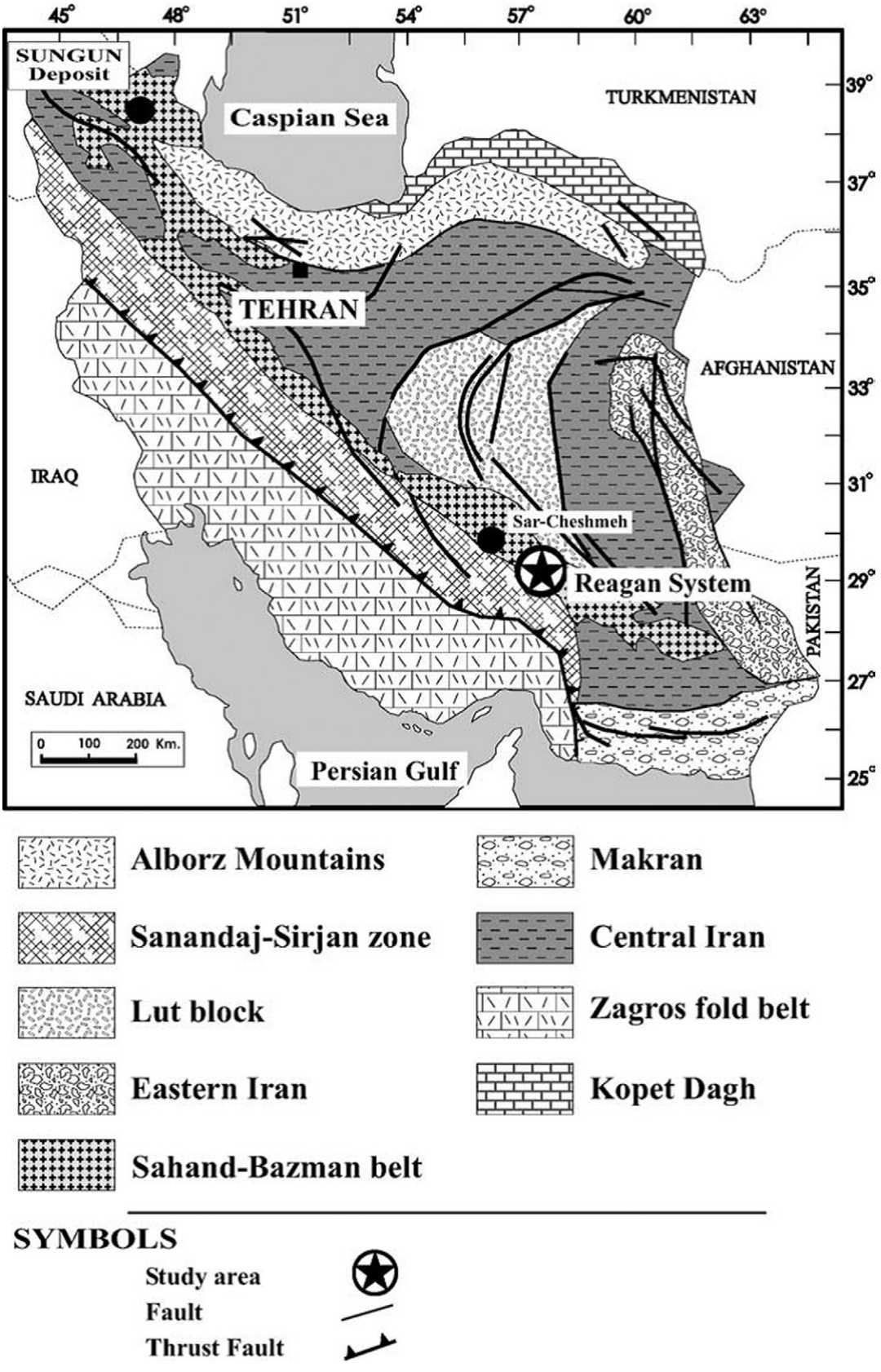

Fig. 1. Geological map of Iran (modified from (Shahabpour, 1994)) showing major lithotectonic units.

Table 1
Common kernel functions for SVM (Hsu et al., 2010)

Type	Kernel function
Linear	$K(x_i,x_j)=\gamma x_i x_j$
Polynomial	$K(x_i,x_j)=(\gamma x_i x_j+r)^d, \gamma>0$
Radial Basis	$K(x_i,x_j)=\exp\{-\gamma\|x_i-x_j\|^2\}, \gamma>0$
Sigmoid	$K(x_i,x_j)=\tanh(\gamma x_i x_j+r), \gamma>0$

therefore, a regression function can be defined in this feature space as follows (Zhang et al., 2011):

$$f(x)=w^T.\varphi(x)+b \tag{1}$$

where w is the weight and b is a constant threshold.

If the insensitive loss function ε is adopted, the aim of SVR is to look for an $f(x)$ which can make the difference between the true and the training values less than the given error ε. Thus, function f solution can be expressed as the following quadratic programming problem:

$$\begin{cases} Min\dfrac{1}{2}w^Tw+C\sum_{i=1}^{l}(\xi_i-\xi_i^*) \\ s.t.\ \ y_i-w.\varphi(x_i)-b\le\varepsilon+\xi_i \\ \quad w.\varphi(x_i)+b-y_i\le\varepsilon+\xi_i^* \\ \quad\quad \xi_i\ge 0 \\ \quad\quad \xi_i^*\ge 0 \end{cases} \tag{2}$$

where C is the error penalty parameter.

Introducing Lagrange multiplier and using the kernel function $K(x_i,x_j)=\varphi(x_i).\varphi(x_j)$ to replace the inner product operation of feature space, the optimization problem of Eq. (2) can be translated into a dual problem as follows:

$$\begin{cases} Max\left[-\dfrac{1}{2}\sum_{i=1}^{l}\sum_{j=1}^{l}(\alpha_i-\alpha_i^*)\left(\alpha_j-\alpha_j^*\right)K(x_i,x_j)-\varepsilon\sum_{i=1}^{l}(\alpha_i-\alpha_i^*)+\sum_{i=1}^{l}y_i(\alpha_i-\alpha_i^*)\right] \\ \quad s.t.\ \sum_{i=1}^{l}(\alpha_i-\alpha_i^*)=0,\qquad i=1,\ldots,l \\ \quad\quad 0\le\alpha_i\le C \\ \quad\quad 0\le\alpha_i^*\le C \end{cases} \tag{3}$$

Solving the dual problem yields the solution of Eq. (1) as follows:

$$f(x)=\sum_{x_i\in SV}(\alpha_i-\alpha_i^*)K(x_i,x)+b \tag{4}$$

where α_i and α_i^* are Lagrange Multipliers, and the non-zero weight samples α_i and α_i^* are called Support Vectors. More common kernel functions are given in Table 1; γ,r, and d in this Table are the kernel parameters. The kernel function selection depends on both the problem nature and type of the data (Hsu et al., 2010); in this study RBF (radial basis function) has been selected as the kernel function because it can, compared with other kernel functions, appropriately analyze high dimensional data sets. Also, compared with other functions (e.g. polynomial functions), it has fewer parameters (γ is the only kernel parameter) resulting in less model complexity (Lin et al., 2008; Che and Hu, 2008; Hsu et al., 2010). In the SVR method, the model parameters include γ (kernel parameter), C (error penalty), and ε (insensitive loss); selection and determination of the optimum value of each one highly affects the SVR model efficiency (Momma and Bennett, 2002; Bao and Liu, 2006). In this research, use was made of the standard SVR method explained in Vapnik (1995).

3.2. Data set

A number of researchers have done detailed studies on fluid inclusion characteristics at Sungun PCD. Hezarkhani and Williams-Jones (1998); Calagari (2004) and Asghari and Hezarkhani (2008) have studied the physico-chemical conditions, mineralization and alteration zones based on fluid inclusion data. In this study, a total of 173 fluid inclusion data sets including attributes as geographic coordinates (longitude, latitude, altitude), thermodynamic parameters (homogenization temperature, eutectic temperature, salinity), type and origin of fluid inclusions were obtained from 59 locations. Table 2 shows the statistical parameters of the fluid inclusion data sets and Fig. 2 shows the histograms of the homogenization temperature, eutectic temperature and salinity. To maintain statistical consistency, the data were divided into training and testing sets, whereby 138 sets (approximately 80%) were used for training and 35 sets (approximately 20%) were chosen for testing. The statistical parameters of the training and testing data sets for thermodynamic parameters (homogenization temperature, eutectic temperature and salinity) are given in Tables 3, 4 and 5, respectively.

4. Results and discussion

4.1. Results of SVR modeling

In this paper, the RBF has been considered as the kernel function for estimating the thermodynamic parameters using the SVR method. To determine the optimum values of γ, ε, and C, use has been made of the grid search method (Hsu et al., 2010) in two steps based on the 4-fold cross validation. In the grid search method, first a coarse grid is formed in the parameter space and then, by getting closer to the optimum point, the grids become finer, and, finally, it gets closer to the global optimum point in the space of the parameter being searched (Momma and Bennett, 2002; Hsu et al., 2010; Lee and Chern, 2013). Therefore, based on this method, first the value of parameter γ is assumed to be constant and then the optimum values of parameters ε and C are calculated in the coarse and fine grids using the grid search method. Next, one of the values found for ε and C in step one is assumed constant, and the optimum value for parameter γ is calculated through the same procedure. Table 6 shows the search range for every model parameter in estimating the homogenization and eutectic temperatures and salinity.

After determining the optimum values of C, γ and ε for the thermodynamic parameters (Table 7) through the grid search method based on

Table 2
Descriptive statistics of fluid inclusion data sets.

Type	LVHS1						LVHS2					
Origin	P			S			P			S		
Parameters	Th	Te	S	Th	Te	S	Th	Te	S	Th	Te	S
Median	387	−48.4	44.8	260	−46.8	37.2	423.2	−53.7	45.1	342.5	−44.1	31.8
Average	382.8	−48.0	44.2	266.7	−48.2	37.3	407.1	−54.3	43.7	342.5	−44.1	31.8
Minimum	294.4	−58	35.9	211	−58	34	250	−66	20	290	−51.2	27
Maximum	499.4	−37.7	56.5	352.6	−44	41.0	466.6	−49.6	54.5	395	−37	36.7
Variance	2000.5	26.4	21.4	2548.0	26.2	7.5	5390.8	30.2	136.0	5512.5	100.8	46.8
Std	44.7	5.1	4.6	50.5	5.12	2.7	73.4	5.5	11.6	74.2	10.0	6.8

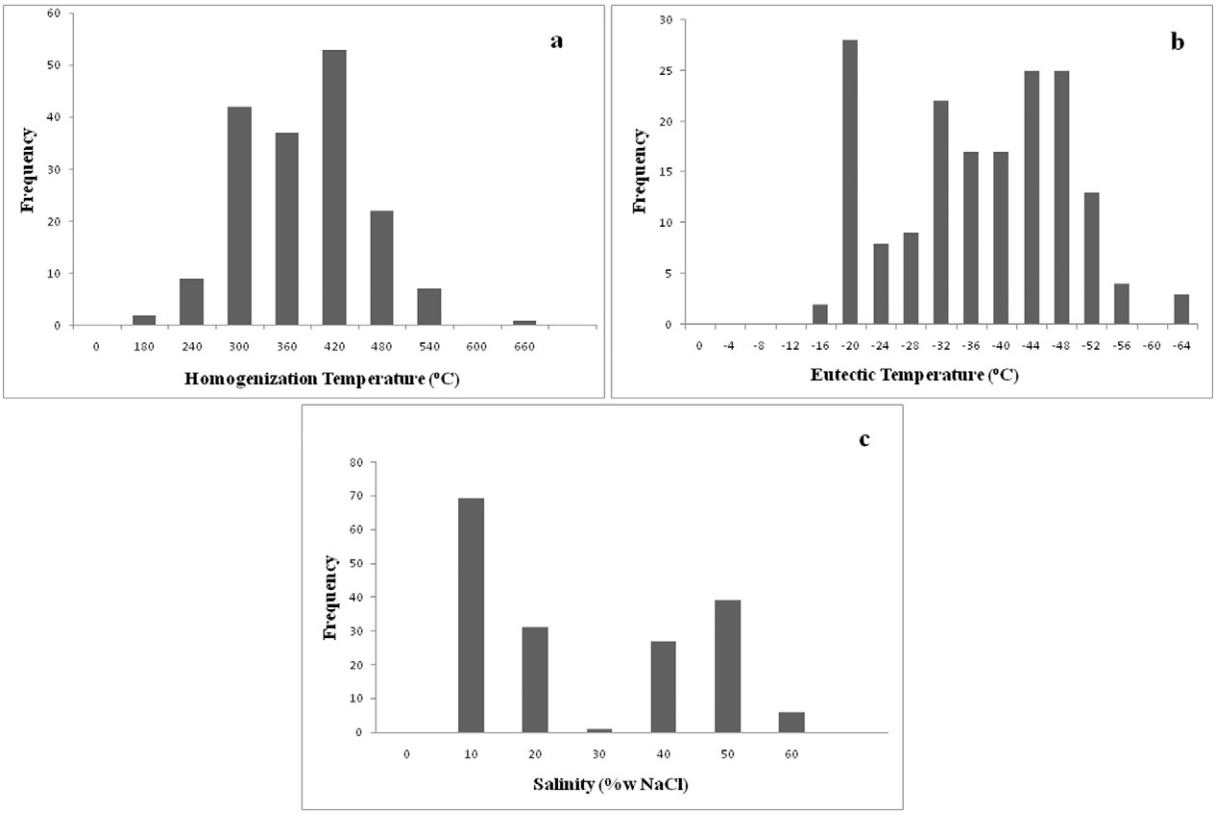

Fig. 2. Histograms of fluid inclusion thermodynamic parameters in Sungun PCD. a) homogenization temperature, b) eutectic temperature and c) fluid salinity.

the 4-fold cross-validation, they were utilized to train the SVR model. Training was performed using the LIBSVM function (Chang and Lin, 2011) in the Weka software based on the optimum parameters, and then the SVR model performance and efficiency were evaluated based on the test data set. Table 8 shows the SVR model results of salinity and temperature parameters for the training and test data sets. As shown, the correlation coefficient for these sets in every mentioned parameter has a favorable value meaning that the model is quite efficient.

The 3D wireframe model of the study area was created using geoscience datasets collected from geological objects and metallogenic features, including a 1:1000 geological map, 1:2500 geological exploration cross-sections, a 1:1000 digital elevation model, 49786 m logs from 156 boreholes (Fig. 3). 3D block model was constructed by filling the wireframe model by 50 m × 50 m × 50 m cells. Then, based on the SVR trained model for different fluid inclusion types and origins, the homogenization and eutectic temperatures and salinity parameters have been estimated.

Fig. 4 shows the SVR model results for the estimation of homogenization and eutectic temperatures and the salinity parameters in the study area using data for fluid inclusions of type $LVHS_1$ with a primary origin.

4.2. Definition of predictive model

Favorable conditions for chalcopyrite deposition in Sungun PCD are 300–400 °C temperature and moderate-to-high salinities (Hezarkhani and Williams-Jones, 1998). Considering favorable thermodynamic conditions for copper deposition, and studying fluid inclusions with different origins and types, the chalcopyrite deposition possibility index in any arbitrary block v based on the fluid inclusion type A and origin B can be defined as follows:

$$K_{AB}(v) = \begin{cases} 1 & \text{if} \quad 300 \le Th_{AB}(v) \le 400 \;\&\; Salinity_{AB}(v) \ge 27 \\ 0 & \text{otherwise} \end{cases} \tag{5}$$

LVHS3						LV						VL					
P			S			P			S			P			S		
Th	Te	S	Th	Te	S	Th	Te	S	Th	Te	S	Th	Te	S	Th	Te	S
381.5	−46.2	44.6	292.5	−47.3	37.4	361.4	−36.5	7.9	277.4	−23	7.3	408.7	−34.9	8.5	299.5	−30.4	5.4
378.9	−46.6	43.1	299.3	−47.6	37.7	370.8	−35.8	8.5	275.1	−27.7	7.9	420.1	−35.2	10.5	298.4	−31.5	6.6
285.4	−67.4	35.7	215	−65	31	180	−53	2.9	162	−55	1.5	334	−56.6	2	219	−43.7	3.5
504	−33.7	52.2	376.5	−33	44.9	527.5	−20.45	18	340.4	−19	18.3	614.5	−23.2	48	375.5	−21.6	12.1
3153.3	42.6	23.7	2605.5	83.7	15.7	6199.9	68.8	16.3	1362.1	79.0	12.1	3924.5	62.7	74.7	7683.9	84.0	14.5
56.1	6.5	4.8	51.0	9.1	3.9	78.7	8.3	4.03	36.9	8.8	3.48	62.6	7.9	8.6	87.6	9.2	3.8

Table 3
Statistical summary of training and test data sets for homogenization temperature.

Parameters	Average		Standard deviation	
	Train	Test	Train	Test
X	8715.762	8742.854	261.3352	250.4698
Y	4872.975	4894.786	188.4147	203.7156
Z	1751.323	1743.671	108.6398	109.6259
Type	3.478261	3.457143	1.576365	1.578213
Origin	0.644928	0.657143	0.480279	0.481594
Th	351.1158	354.0206	78.49633	80.55705

On this basis, for every block v from the 3D block model, 10 K_{AB} indices can be defined and determined. For example, Fig. 5 shows the 3D model of chalcopyrite deposition possibility index for fluid inclusion type $LVHS_1$ with primary origin.

Investigating K-based models is very complicated, if not impossible, due to the large number of the models presentable on this basis. For simplicity, the following mineralization possibility indices can be defined based on different fluid inclusion populations:

$$\begin{aligned} I_{Population I}(v) &= \sum_{A\in Population\ I}\ \sum_{B\in\{P,S\}} K_{AB}(v) \\ I_{Population II}(v) &= \sum_{A\in Population\ II}\ \sum_{B\in\{P,S\}} K_{AB}(v) \\ I_{Population III}(v) &= \sum_{A\in Population\ III}\ \sum_{B\in\{P,S\}} K_{AB}(v) \end{aligned} \quad (6)$$

Based on these indices, favorable areas are specified in 3D models, which are defined as the "predictive models". Blocks in the predictive models that have the possibility of chalcopyrite mineralization for at least one of the populations ($I_{Population\ I}+I_{Population\ II}+I_{Population\ III}\geq 1$) were defined as high prospectivity zones and the others as low prospectivity zones. Fig. 6 shows a cross section of the predictive models for different populations of fluid inclusions.

To evaluate the efficiency of the SVR model, the obtained predictive models were compared with the 3D model of the copper grade (Fig. 6). Block grade values were estimated employing ordinary block kriging technique using the double-structure spherical semi-variogram model (with the parameters nugget effect = 0, sill of first structure = 0.07, sill of second structure = 0.05, range of first structure = 71.5 m, and range of second structure = 208 m). To make the comparison of the predictive and grade models possible, the grade block model was classified, based on the geological cutoff grade, into "ore" and "waste"; results of the comparison of the predictive and grade block models are given in Table 9. As shown, the 505 blocks estimated as "low prospectivity" in the predictive model correspond to the "waste" in the copper grade model, and the 11799 blocks estimated as "high prospectivity" in the predictive model correspond to "ore" in the grade block model. Therefore, in 82% of the cases, classification of low and high prospectivity zones based on the predictive model (prepared based on 173 fluid inclusions data) conforms to that of the grade block model (prepared based on 25381 assay data).

Table 4
Statistical summary of training and test data sets for eutectic temperature.

Parameters	Average		Standard deviation	
	Train	Test	Train	Test
X	8730.504	8742.511	258.4936	259.8533
Y	4880.964	4880.343	191.8663	195.406
Z	1750.223	1750.806	109.758	109.3634
Type	3.449275	3.428571	1.566401	1.650057
Origin	0.644928	0.657143	0.480279	0.481594
Te	−38.8101	−38.6299	11.29765	11.2906

Table 5
Statistical summary of training and test data sets salinity.

Parameters	Average		Standard deviation	
	Train	Test	Train	Test
X	8718.617	8731.599	258.1663	264.259
Y	4876.087	4882.514	192.6572	187.9957
Z	1739.741	1789.34	107.3948	105.4968
Type	3.434783	3.628571	1.584397	1.535573
Origin	0.652174	0.628571	0.478016	0.490241
Salinity	22.80229	22.68831	17.50262	17.61572

To schematically compare the predictive and copper grade models, cross sections of these models are shown in Fig. 6. As shown, there is high potential of chalcopyrite mineralization based on the SVR-based predictive models for populations I and II. The model prepared based on population III shows mineralization potential only in a small part but not in a major part of the region. A comparison of the SVR-based predictive models with the copper grade block model shows acceptable conformity in low, moderate, and high grade regions. It should be noted, however, that expecting full conformity is quite strict and almost impossible because the number of fluid inclusion data (173) is small compared with that of the copper grade (25381). For instance, the predictive model shows high mineralization potential in deep regions of the eastern parts but the copper grade model does not confirm it. The main reason can be attributed to the fact that the drilling spacing in this part is large (about 200 m) showing a small number of drillholes compared to the central and western parts.

4.3. Locating additional drillholes based on predictive models

Considering high drilling costs, the number of additional drillholes is usually specified based on budget limitations, and the company is willing to drill more drillholes in zones with high mineralization probability and the fewest possible in the waste.

Fluid inclusions provide information on the genesis of mineral deposits and also is a strong tool applied for mineral exploration. Based on fluid inclusion homogenization temperatures, it is possible to calculate the exact local pressure (both lithostatic and hydrostatic pressures), evident for the different zones of mineralization. It also let us know about the possible location of hidden masses of main mineralization (Hezarkhani, 1997; Hezarkhani and Williams-Jones, 1998). Therefore, preparing a predictive model based on these information can be effective in confining the mineralization zone and, hence, in reducing the exploration budget. Based on these models, it is possible to specify the places where deeper drillholes are required (or not required at all)

Table 6
The search range for every model parameter in estimating the homogenization and eutectic temperatures and the fluid salinity taken from (Frohlich and Zell, 2005; Hsu et al., 2010).

the SVR model parameters	Range search
C	$\{2^{15},\ldots\ldots,2^{5}\}$
γ	$\{2^{3},\ldots\ldots,2^{-15}\}$
ε	$\{2^{-1},\ldots\ldots,2^{-8}\}$

Table 7
The optimum values of parameters C, γ and ε for the homogenization and eutectic temperatures and the fluid salinity.

Optimum values of parameters	Th	Te	Salinity
C	9742	90.5	2435.5
γ	0.03125	0.5	0.210224
ε	0.84	0.015625	0.0078125

Table 8
The SVR model results of salinity and temperature parameters for the training and test data sets.

LIBSVM	Th		Te		Salinity	
	Train	Test	Train	Test	Train	Test
Correlation Coefficient	0.7019	0.765	0.7808	0.7142	0.9566	0.9261
RMSE	55.8133	52.4269	7.0585	7.9698	5.1166	6.6454
No. of data	138	35	138	35	138	35

before drilling; for instance, drillhole BH135 (which is additional) on cross section 4600N of the predictive model (Fig. 7). Fig. 8a shows the copper grade variations against depth of the samples taken from drillhole BH135. As shown, despite costs incurred to drill this drillhole, most of it has been drilled in parts where the copper grade is quite low. Based on the predictive model (Fig. 7), this borehole has been drilled in a low potential zone and drilling operations have been terminated before reaching high potential zones. If drilling pattern was planned based on the predictive model, the efficiency would increase with an increase in the borehole depth. On the other hand, studying the location of borehole BH145 shows that although its initial parts have been drilled in a low potential zone, it is possible that it will intersect higher potential zones too because it has an appropriate depth (Fig. 7). According to Fig. 8b, samples taken from this borehole conform appropriately to the predictive model. Next, effort was made to plan a pattern of additional drillholes based on the predictive models wherein the location and especially the proposed depths are determined based on the extension of high potential zones (Fig. 9). For this purpose, use was made of the following algorithm:

1—Draw the probable boundaries of the mineralization zone based on the predictive model.

2—Specify the location of the additional drillholes based on the drilling density and boundaries drawn in step 1.

3—Determine the depth of each additional drillhole based on the vertical variations of the predictive model.

In step 1, in each cross-section of the predictive model, the boundaries of the zones having a potential of mineralization are specified and then the probable boundary of the mineralization zone is drawn through interpolation between cross-sections (dotted line in Fig. 9). In step 2, if a regular pattern is desired, its dimensions are specified based on the vastness of the mineralization zone and the number of additional drillholes. But, if an optimal locating of the drillholes (based on a specific objective function) is desired, it is possible to use simulated annealing-based or genetic-algorithm based procedures for the purpose; more details of such algorithms are provided in Soltani and Hezarkhani (2011 and Soltani and Hezarkhani, 2013a,Soltani-Mohammadi and Hezarkhani, 2013b). To make the comparison with Sungun drilling results possible, the additional drilling pattern was designed and its dimensions were considered equal to those of Sungun deposit pattern. Then, based on the vertical variability of the predictive model, step 3 involved approximation of depth for each additional drillhole. Fig. 9 shows the location and depth proposed for each additional drillhole based on the above algorithm. Considering the high mineralization potential in the eastern part (based on the predictive model), 22 drillholes with minimum depths of 200 m each, 3 with minimum depths of 300 m each, and 1 with minimum depth of 400 m have been proposed. The predictive model predicts that mineralization potential is high in the central parts and increases as the depth increases. This is why 13 drillholes with minimum depths of 600 m each and 33 with minimum depths of 300 m each have been suggested. Again, mineralization potential is, according to the predictive model, low in surface areas of the western part, but with an increase in depth, this potential increases too; therefore, 4 drillholes with depths more than 400 m each and 4 with depths more than 300 m each have been proposed.

In Sungun area, 9 actual additional drillholes (1–9 in Fig. 3) have been drilled in locations that are, according to the predictive model, low potential zones; 6% of the total drilling cost in this area goes for these 9 actual additional drillholes. In the proposed drilling pattern based on the predictive model, no additional drillhole has been suggested in this part, but, instead, 9 additional drillholes have been suggested in high potential zones. It is to be noted that even if these proposed additional drillholes are drilled, some of them may not

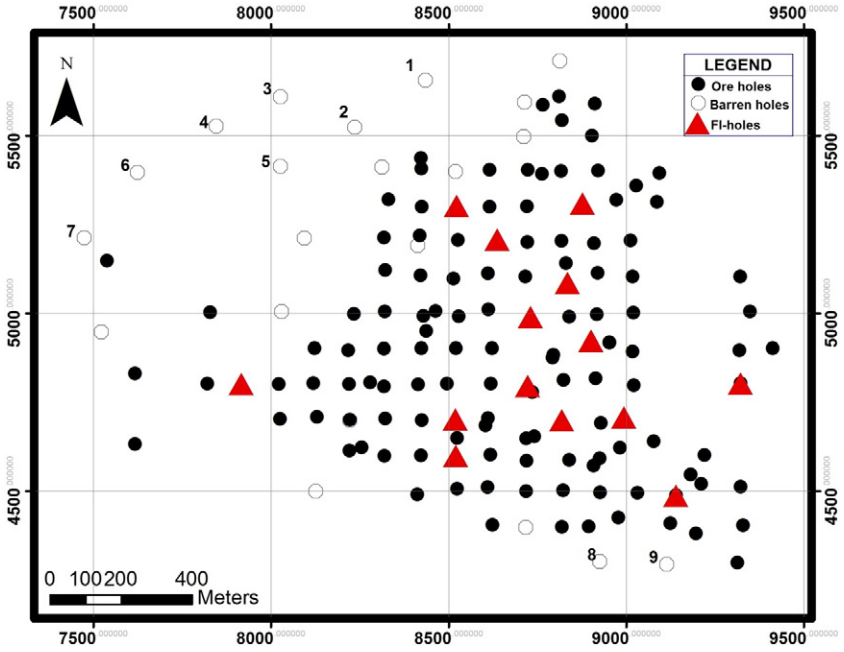

Fig. 3. Drilling pattern in the Sungun area. Open symbols indicate barren holes and filled indicate ore holes. Locations of the initial drillholes from which the fluid inclusion samples have been taken (FI-holes) are shown with solid red triangles.

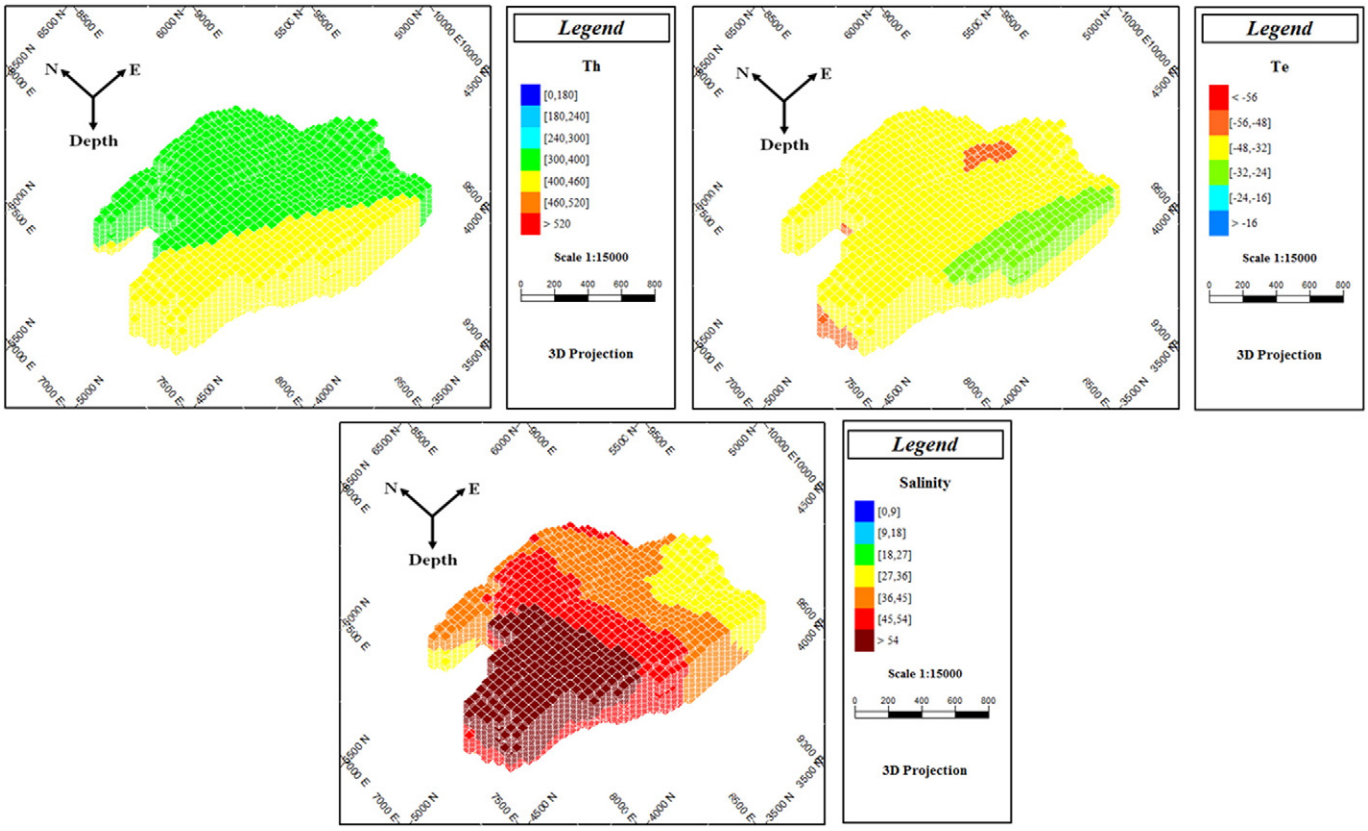

Fig. 4. The SVR model results for the estimation of homogenization and eutectic temperatures and the fluid salinity parameters in the study area for the fluid inclusion of type LVHS1 with a primary origin.

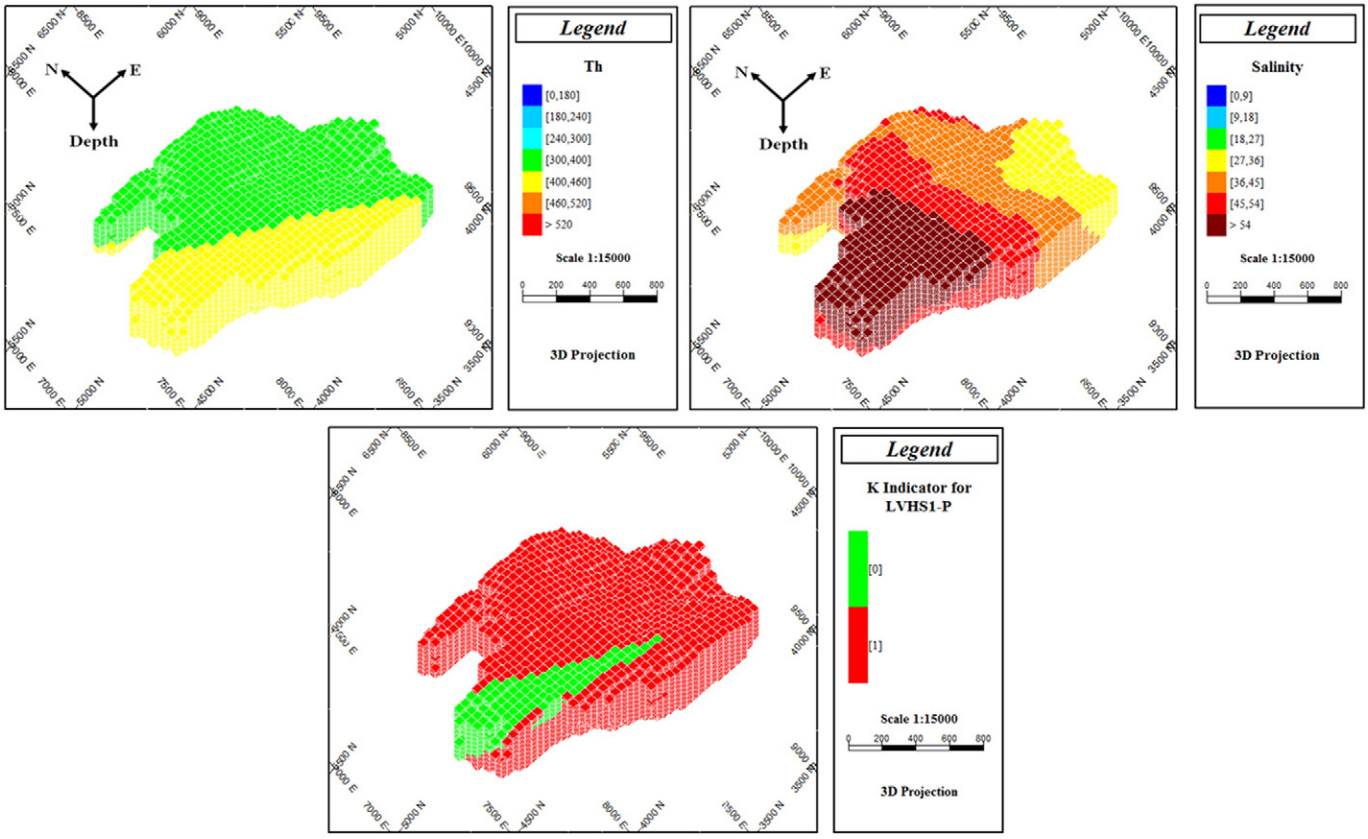

Fig. 5. The 3D model of the chalcopyrite deposition possibility index for fluid inclusion type LVHS1 with primary origin.

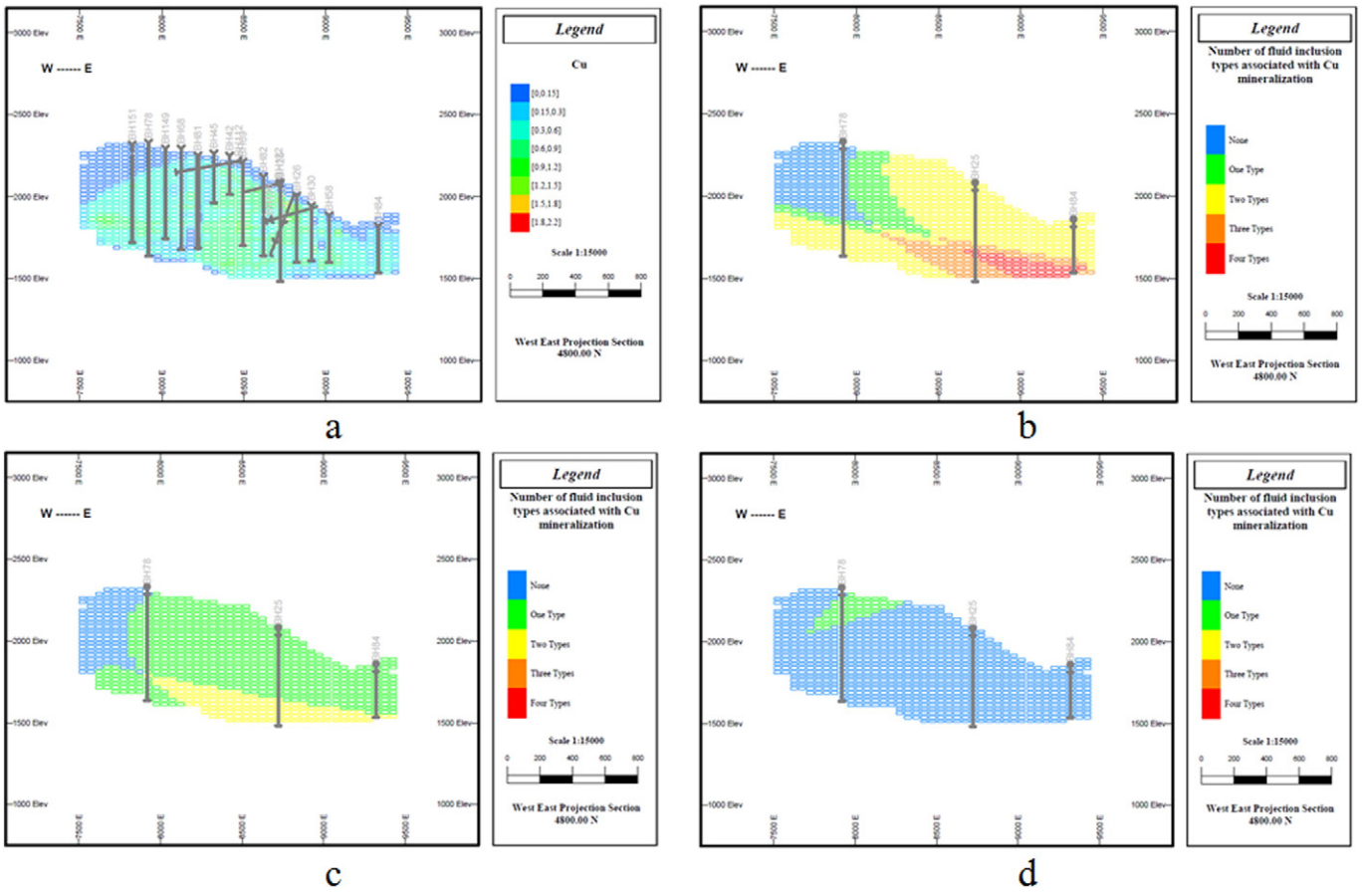

Fig. 6. Comparison of 3D predictive models for different populations of fluid inclusions with the 3D model of the copper grade, a) the 3D model of the copper grade, b) the 3D predictive model for fluid inclusion population I, c) the 3D predictive model for fluid inclusion population II, d) the 3D predictive model for fluid inclusion population III.

intersect ore deposit; they can be used to determine the boundary of deposit more precisely.

As shown in Fig. 10, locations of some drillholes in both the existing and proposed patterns almost coincide and sufficient data have been obtained from those points.

Since grade variability is low in this copper deposit (the range of the model fitted to the experimental variogram of the copper grade is 208 m), and drilling costs are high, it is possible to avoid the drilling of those drillholes (in the proposed pattern) 137 m ($\frac{2}{3}\times$ range) from which there are at least 4 drillholes in the existing pattern or those the distances of which are less than 10 m. Therefore, it is suggested that, if conditions are appropriate for the development of the exploration operations, the additional drilling be carried out only in other points of the proposed pattern (in Fig. 10, letter R has been put over them). In some other points, the number of drillholes in the existing pattern is enough, but it is necessary, based on the proposed pattern, to drill deeper drillholes in their around; in Fig. 10, such cases are marked with L1–L5. For instance, the necessity of increasing the exploration depth at point L5 (next to drillhole BH135) is shown in Fig. 7.

Table 9
Results of validation of prospectivity modeling

		Grade block model	
		Waste	Ore
Predictive model	Low Prospectivity Zone	505	195
	High Prospectivity Zone	2543	11799

5. Conclusions

Studies carried out so far on fluid inclusion data have mostly dealt with physicochemical modeling and modeling of alteration zones in the 2D space and have led to the discrimination of such zones in porphyry deposits. Effort has been made in this paper, for the first time, to do 3D modeling of the fluid inclusion data using SVR in order to estimate the thermodynamic parameters that affect mineralization. A comparison of the SVR-based predictive model and the copper grade block model shows an acceptable conformity in low, moderate, and high grade regions. However, full correlation is quite strict and almost impossible due to the small number of the fluid inclusion data compared to those of the copper grade. This correlation can be used to evaluate the existing exploratory drilling in the area and check the effects of using predictive models on advancing the process of detailed explorations.

Since, in this paper, the efficiency of the predictive model obtained from the 3D modeling of the fluid inclusion data have been used only in Sungun porphyry copper deposit, it is suggested that the future studies may focus on the efficiency of this model in advancing the exploration process of other porphyry copper deposits, lead, zinc, and hydrocarbon reserves so as to enable more certain decision making regarding the model efficiency. The fluid inclusion data are not limited to only the homogenization and eutectic temperatures and salinity, other valuable data such as the fluid inclusion composition is also quite useful.

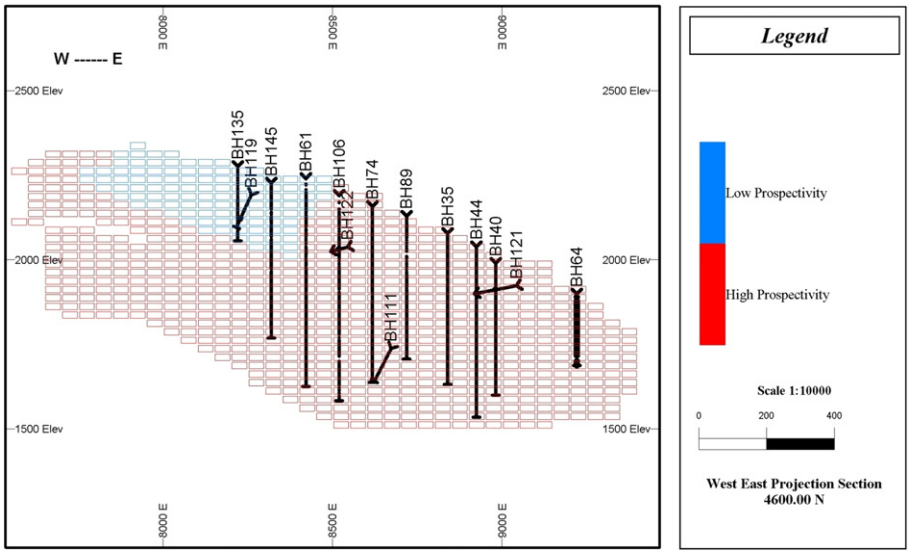

Fig. 7. Cross-section 4600N showing distribution of low and high prospectivity zones in the predictive model and drillholes.

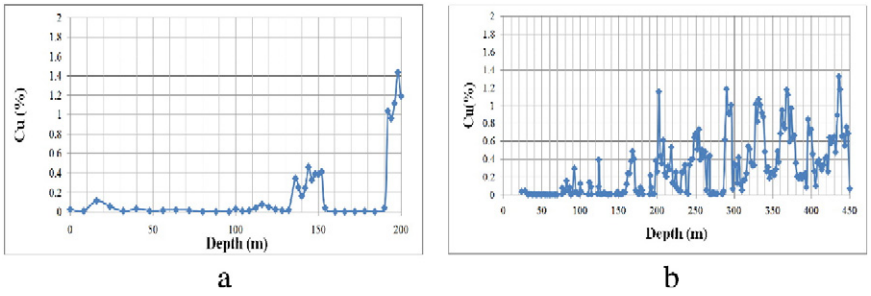

Fig. 8. Variation of Cu grade with Depth for drillholes a) BH135 and b) BH145.

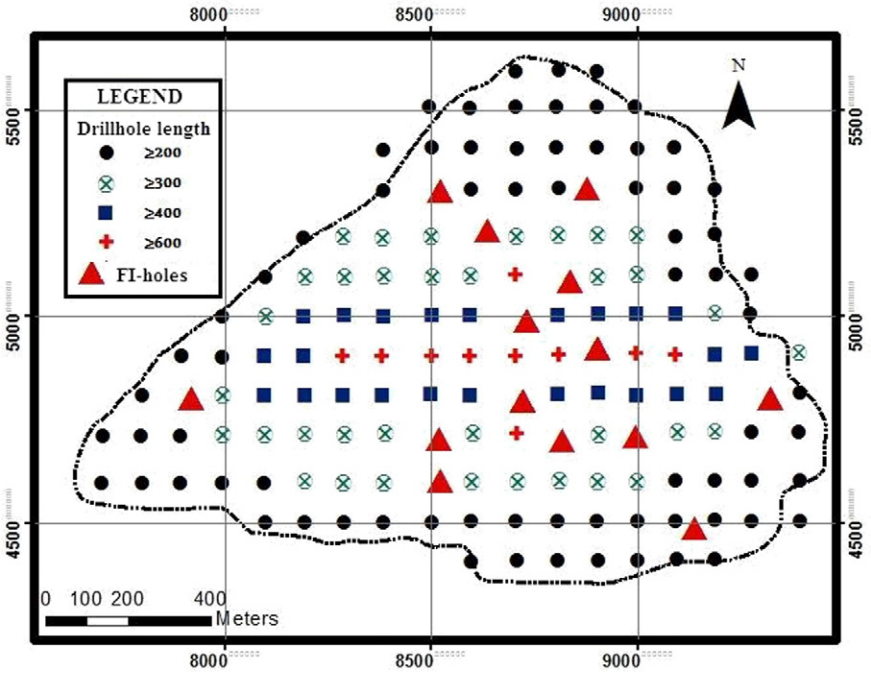

Fig. 9. Proposed drilling pattern based on the predictive model.

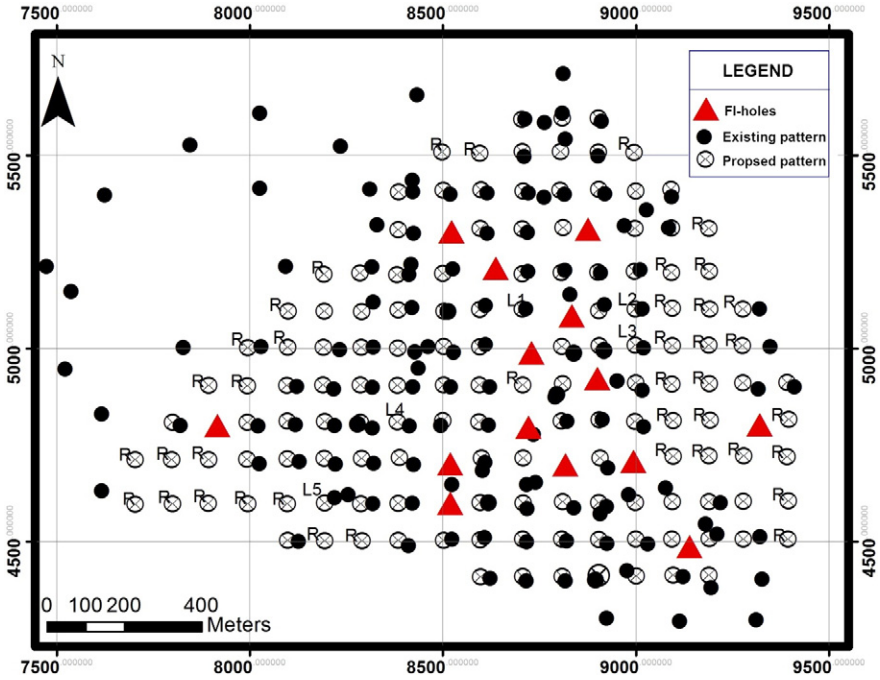

Fig. 10. Comparison of the drilled and proposed patterns based on the predictive model. The proposed, high priority additional drillholes, and those the drilling of which is necessary to increase the exploration depth are shown with letters R and L respectively.

Since the latter was inaccessible in Sungun porphyry copper deposit, it was neglected in the present study. It is suggested that the modeling input data be increased through the use of the data of the well-known deposits in the world wherein the number of fluid inclusion samples is more and the data are gathered uniformly by a team.

Acknowledgments

The authors are indebted to Prof. John Carranza and the anonymous reviewers for their valuable comments on an earlier draft of this paper.

References

Abbaszadeh, M., Hezarkhani, A., Soltani-Mohammadi, S., 2013. An SVM based machine learning method for the separation of alteration zones in Sungun porphyry copper deposit. Chem. Erde-Geochem. 73, 545–554.

Abbaszadeh, M., Hezarkhani, A., Soltani-Mohammadi, S., 2015. Classification of alteration zones based on whole-rock geochemical data using support vector machine. J. Geol. Soc. India 85.

Abdollahi, M.J., Karimpour, M.H., Kheradmand, A., Zarasvandi, A.R., 2009. Stable isotopes (O, H, and S) in the Muteh gold deposit, Golpaygan area, Iran. Nat. Resour. Res. 20, 157–176.

Al-Anazi, A., Gates, D., 2010. On the capability of support vector machines to classify lithology from well logs. Nat. Resour. Res. 19, 125–139.

Asghari, O., Hezarkhani, A., 2008. Applying discriminant analysis to separate the alteration zones within the Sungun porphyry copper deposit. J. Appl. Sci. 24, 4472–4486.

Bakker, R.J., 1999. Optimal interpretation of microthermometrical data from fluid inclusions: thermodynamic modelling and computer programming (Habilitation thesis) Univ Heidelberg, Germany.

Bao, Y., Liu, Z., 2006. A fast grid search method in support vector regression forecasting time series. intelligent data engineering and automated learning — IDEAL 2006. Lect. Notes Comput. Sci 4224, 504–511.

Beane, R.E., Bodnar, R.J., 1995. Hydrothermal fluids and hydrothermal alteration in porphyry copper deposits. In: Pierce, F.W., Bohm, J.G. (Eds.), Porphyry Copper Deposits of the American Cordillera: TucsonAZAZ Geol. Soc. Dig. 20. Arizona Geological Society, Arizona, United States, pp. 83–93.

Beane, R.E., Titley, S.R., 1981. Porphyry copper deposits, Part II: hydrothermal alteration and mineralization. Econ. Geol. 75, 235–269.

Calagari, A.A., 2003. Stable isotope (S, O, H and C) studies of the phyllic and potassic–phyllic alteration zones of the porphyry copper deposit at Sungun, East Azarbaidjan, Iran. J. Asian Earth Sci. 21, 767–780.

Calagari, A.A., 2004. Fluid inclusion studies in quartz veinlets in the porphyry copper deposit at Sungun, East-Azarbaidjan, Iran. J. Asian Earth Sci. 23, 179–189.

Canet, C., Franco, S.I., Prol-Ledesma, R.M., González-Partida, E., Villanueva-Estrada, R.E., 2011. A model of boiling for fluid inclusion studies: application to the Bolaños Ag–Au–Pb–Zn epithermal deposit, Western Mexico. J. Geochem. Explor. 110, 118–125.

Chang, C.C., Lin, C.J., 2011. LIBSVM: a library for support vector machines. ACM Trans. Intell. Syst. Technol. 2, 1–27.

Chatterjee, S., Bandopadhyay, S., 2011. Goodnews Bay Platinum resource estimation using least squares support vector regression with selection of input space dimension and hyperparameters. Nat. Resour. Res. 20, 117–129.

Che, X.L., Hu, L., 2008. Grid resource prediction approach based on Nu-support vector regression. Proceedings of the Seventh International Conference on Machine Learning and Cybernetics, Kunming, 12–15 July, pp. 778–783.

Chou, D., Schenk, D.E., 1983. Optimum locations for exploratory drill holes. Int. J. Min. Eng. 1, 343–355.

Drew, k.J., 1974. Estimation of petroleum exploration success and the effects of resource base exhaustion via a Simulation model: U.S. Geol. Survey Bull 1328 (25 pp.).

Dutta, S., 2006. Predictive performance of machine learning algorithms for ore reserve estimation in sparse and imprecise data (PhD thesis) University of Alaska Fairbanks (189 pp.).

Dutta, S., Bandopadhyay, S., Ganguli, R., Misra, D., 2010. Machine learning algorithms and their application to ore reserve estimation of sparse and imprecise data. J. Intell. Learn. Syst. Appl. 2, 86–96.

El-Makky, A.M., 2011. Statistical analyses of La, Ce, Nd, Y, Nb, Ti, P, and Zr in bedrocks and their significance in geochemical exploration at the Um Garayat gold mine area, Eastern Desert, Egypt. Nat. Resour. Res. 20, 157–176.

Frohlich, H., Zell, A., 2005. Efficient parameter selection for support vector machines in classification and regression via model-based global optimization. Proceedings of the International Joint Conference on Neural Networks, (IJCNN '05), IEEE, Montreal, Quebec, Canada, pp. 1431–1436.

Geranian, H., Tabatabaei, S.H., Asadi, H.H., Carranza, E.J.M., 2015. Application of discriminant analysis and support vector machine in mapping gold potential areas for further drilling in the Sari-Gunay Gold Deposit, NW Iran. Nat. Resour. Res. http://dx.doi.org/10.1007/s11053-015-9271-2.

Gershon, M.E., 1983. Optimal drillhole location using geostatistics. In Preprint — Society of Mining Engineers of AIME. Soc of Mining Engineers of AIME, Littleton, Colo, USA.

Hassani Pak, A.A., Sharafodin, M., 2004. GET: a function for preferential site selection of additional borehole drilling. Explor. Min. Geol. 13, 139–146.

Hezarkhani, A., 1997. Physicochemical Controls on Alteration and Copper Mineralization in the Sungun Porphyry Copper System, Iran. University of McGill, Montreal, Quebec, Canada.

Hezarkhani, A., 2002. Specific physico-chemical conditions (360 °C) for chalcopyrite dissolution/porphyry system in the Reagan porphyry copper porphyry system, Iran. Amirkabir J. Sci. Technol. 13, 668–687.

Hezarkhani, A., 2003. Hydrothermal evolution in the Raigan porphyry copper system based on fluid inclusion studies, (Kerman, Iran): the path to an uneconomic deposit. Amirkabir J. Sci. Technol. 15, 74–84.

Hezarkhani, A., 2006a. Mineralogy and fluid inclusion investigations in the Reagan Porphyry System, Iran, the Path to an uneconomic porphyry copper deposit. J. Asian Earth Sci. 27, 598–612.
Hezarkhani, A., 2006b. Hydrothermal evolutions at the Sar-Cheshmeh porphyry Cu–Mo deposit, Iran: evidence from fluid inclusions. J. Asian Earth Sci. 28, 408–422.
Hezarkhani, A., 2008b. Hydrothermal evolution in Miduk porphyry copper system (Kerman, Iran): based on the fluid inclusion investigation. Int. Geol. Rev. 50, 665–684.
Hezarkhani, A., 2009. Hydrothermal fluid geochemistry at the Chah-Firuzeh porphyry copper deposit, Iran: evidence from fluid inclusions. J. Geochem. Explor. 101, 254–264.
Hezarkhani, A., Williams-Jones, A.E., 1998. Controls of alteration and mineralization in the Sungun Porphyry Copper Deposit, Iran: evidence from fluid inclusions and stable isotopes. Econ. Geol. 93, 651–670.
Hezarkhani, A., Williams-Jones, A.E., Gammons, C.H., 1999. Factors controlling copper solubility and chalcopyrite dissolution in the Sungun porphyry copper deposit, Iran. Mineral. Deposita 34, 770–783.
Hezarkhani, A., Tahmasebi, T., Asghari, O., 2010. Separating the Sungun copper deposit alteration zones by applying artificial neural network. J. Geosci. 20, 41–46.
Hsu, C.W., Chang, C.C., Lin, C.J., 2010. A practical guide to support vector classification, technical report, department of computer science and information engineering. University of National Taiwan, Taipei.
Jadhav, G.N., Panchapakesan, V., Sahu, K.C., 1993. The role of fluid inclusions in mineral exploration—an attempt on the Bihar Mica Belt of India. Nonrenewable Resour. 2, 156–166.
Kecman, V., 2000. Learnig and soft computing: support vector machines, neural network and fuzzy logic models. MIT Publishers (576 pp.).
Kecman, V., 2004. Support vector machines basics, the university of auckland, school of engineering, report 616.
Kim, Y.C., Martino, F., Chopra, I., 1981. Application of geostatistics in a coal deposit. Min. Eng. 33, 1476–1481.
Koch Jr., G.S., Link, R.F., 1974. A mathematical model to guide the discovery of orebodies in a Coeur d'Alene Lead–Silver Mine: U.S. Bur. Mines Rept. Inv. 7989 (43 pp.).
Landtwing, M.R., Pettke, T., Halter, W.E., Heinrich, C.A., Redmond, P.B., T. E. M., Einaudi, M.T., Kunze, K., 2005. Copper deposition during quartz dissolution by cooling magmatic-hydrothermal fluids: The Bingham porphyry. Earth Planet. Sci. Lett. 235, 229–243.
Lee, C.Y., Chern, S.G., 2013. Application of a Support Vector Machine for Liquefaction Assessmen. J. Mar. Sci. Technol. 21, 318–324.
Lin, S.W., Lee, Z.J., Chen, S.C., Tseng, T.Y., 2008. Parameter determination of support vector machine and feature selection using simulated annealing approach. Appl. Soft Comput. 8, 1505–1512.
Lowell, J.D., Guilbert, J.M., 1970. Lateral and vertical alteration mineralization zoning in porphyry ore deposits. Econ. Geol. 65, 373–408.
Malmqvist, K., Malmqvist, L., Zwiefel, H., 1980. Computer simulation of simulation for deep-seated orebodies in mining districts. Econ. Geol. 75, 927–935.
Momma, M., Bennett, K., 2002. A pattern search method for model selection of support vector regression. SIAM Conf. on Data Mining, pp. 261–274.
Moncada, D., 2008. Application of fluid inclusions and mineral textures in exploration for epithermal precious metals deposits (Msc, Thesis) Virginia Polytechnic Institute and State University.
Moritz, R., 2006. Fluid salinities obtained by infrared microthermometry of opaque minerals: implications for ore deposit modeling — a note of caution. J. Geochem. Explor. 89, 284–287.
Morshedy, A.H., Memarian, H., 2015. A novel algorithm for designing the layout of additional boreholes. Ore Geol. Rev. 67, 34–42.
Morshedy, A.H., Torabi, S.A., Memarian, H., 2015. A new method for 3D designing of complementary exploration drilling layout based on ore value and objective functions. Arab. J. Geosci. 8, 8175–8195.
Pozdnoukhov, A., 2005. Support vector regression for automated robust spatial mapping of neural radioactivity. J. Appl. GIS 1.
Qahwash, A.-L.A., 1987. An optimal algorithm for drilling strategy. Energy 12, 423–425.
Rusk, B.G., Reed, M.H., Dilles, J.H., Klemm, L.M., Heinrich, C.A., 2004. Compositions of magmatic hydrothermal fluids determined LAICP–MS of fluid inclusions from the porphyry copper-molybdenum deposit at Butte, MT. Chem. Geol. 210, 173–199.
Savinskii, I.D., 1965. Probability tables for locating elliptical underground masses with a rectangular grid. Consultants Bureau, New York (110 pp.).
Schuenemeyer, J.H., Bawiec, W.J., Drew, L.L., 1980. Computational methods for a three-dimensional model of the petroleum-discovery process. Comput. Geosci. 6, 323–360.
Shahabpour, J., 1994. Post-mineralization breccia dike from the Sar-Cheshmeh porphyry copper deposit, Kerman, Iran. Explor. Min. Geol. 3, 39–43.
Smola, A.J., Scholkopf, B., 1998. A tutorial on support vector regression. NeuroCOLT Technical Report NC-TR-98-030, Royal Holloway College. University of London, UK.
Smola, A.J., Scholkopf, B., 2004. A tutorial on support vector regression. Stat. Comput. 14, 199–222.
Soltani, S., Hezarkhani, A., 2011. Determination of realistic and statistical value of the information gathered from exploratory drilling. Nat. Resour. Res. 20, 207–216.
Soltani, S., Hezarkhani, A., 2013a. Optimum locating of additional drillholes to optimize the statistical value of information. J. Min. Metall. 49, 21–29.
Soltani Mohammadi, S., Hezarkhani, A., Erhan Tercan, A., 2012. Optimally locating additional drill holes in three dimensions using grade and simulated annealing. J. Geol. Soc. India 80, 700–706.
Soltani, S., Hezarkhani, A., Erhan Tercan, A., Karimi, B., 2011. Use of genetic algorithm in optimally locating additional drill holes. J. Min. Sci. 47, 62–72.
Soltani-Mohammadi, S., Hezarkhani, A., 2013b. A simulated annealing-based algorithm to locate additional drillholes for maximizing the realistic value of information. Nat. Resour. Res. 22, 229–237.
Sun, L., Xiao, K., Gao, Y., Wang, R., Xing, S., 2011. 3D modeling of fluids inclusion data of caixiashan Pb–Zn deposit, East Tianshan Area, China, IAMG2011, Austria.
Szidarovszky, F., 1983. Multi objective observation network design for regionalized variables. Int. J. Min. Eng. 1, 331–342.
Tahmasebi, P., Hezarkhani, A., 2009. Application of discriminant and principal components analysis for alteration separation; sungun copper porphyry deposit, East Azerbaijan, Iran. Aust. J. Basic Appl. Sci. 6, 564–576.
Thiery, R., 2006. Thermodynamic modeling of aqueous CH4-bearing fluid inclusions trapped in hydrocarbon-rich environments. Chem. Geol. 227, 154–164.
Twarakavi, N.C., Misra, D., Bandopadhayay, S., 2006. Prediction of arsenic in bedrock derived stream sediments at a gold mine site under conditions of sparse data. Nat. Resour. Res. 15, 15–26.
Vapnik, V., 1995. The Nature of Statistical Learning Theory. Springer, New York.
Zhang, G.P., Patuwo, B.E., Hu, M.Y., 1998. Forecasting with artificial neural networks: the state of the art. Int. J. Forecast. 1, 35–62.
Zhang, D., Xu, G., Zhang, W., Golding, S.D., 2007. High salinity fluid inclusions in the Yinshan polymetallic deposit from the Le–De metallogenic belt in Jiangxi Province, China: Their origin and implications for ore genesis. Ore Geol. Rev. 31, 247–260.
Zhang, D., Liu, W., Wang, A., Deng, Q., 2011. Parameter optimization for support vector regression based on genetic algorithm with simplex crossover operator. J. Inform. Computat. Sci. 8, 911–920.
Zuo, R., Carranza, E.J.M., 2011. Support vector machine: a tool for mapping mineral prospectivity. Comput. Geosci. 37, 1967–1975.